Volume 13 | Number 21 | 7 June 2017 | Pages 3833–4002

Soft Matter

rsc.li/soft-matter-journal

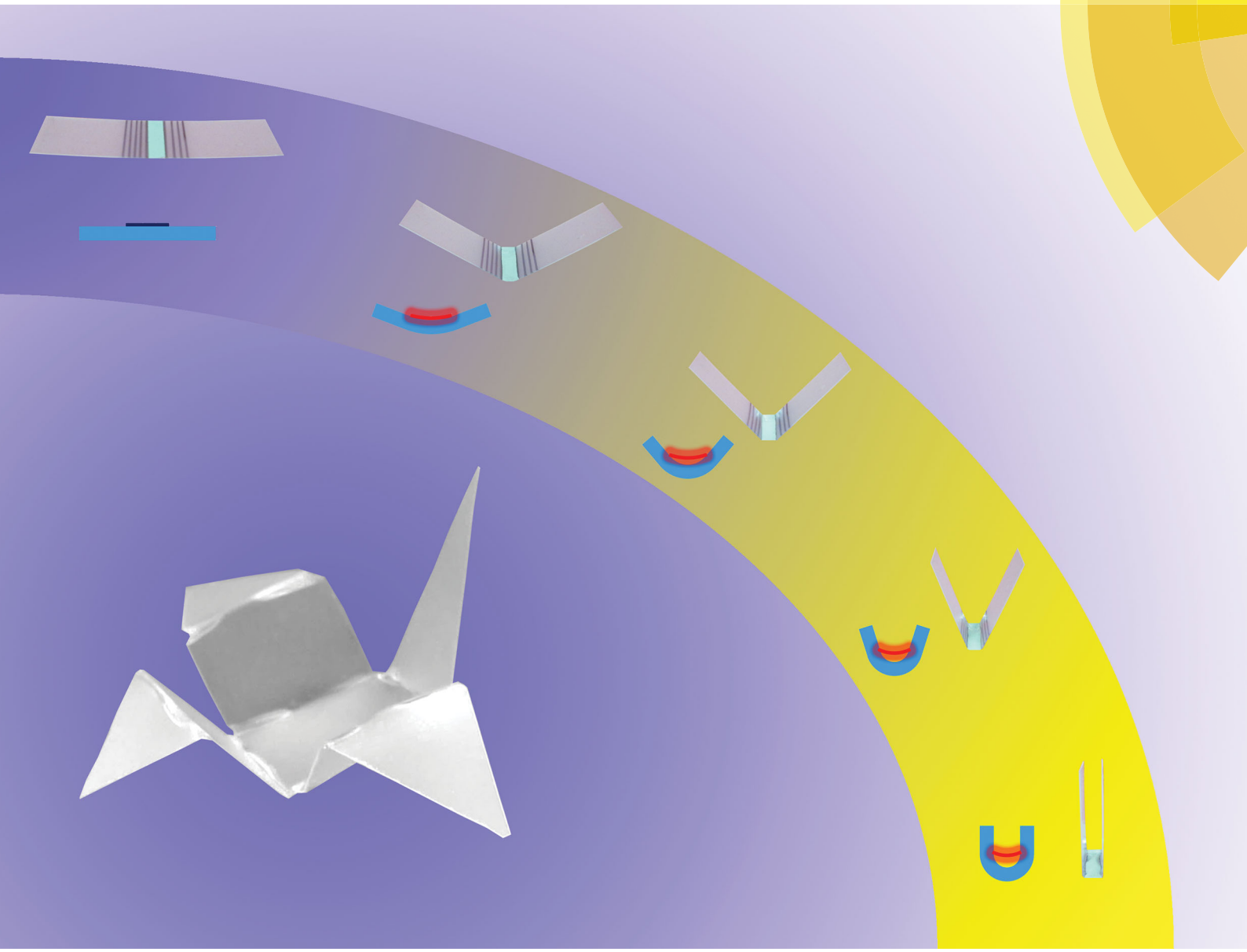

ISSN 1744-6848

ROYAL SOCIETY OF CHEMISTRY

PAPER
Yong Zhu *et al.*
Controlling the self-folding of a polymer sheet using a local heater: the effect of the polymer–heater interface

Soft Matter

PAPER

View Article Online
View Journal | View Issue

Cite this: *Soft Matter*, 2017, **13**, 3863

Controlling the self-folding of a polymer sheet using a local heater: the effect of the polymer–heater interface†

Jianxun Cui, Shanshan Yao, Qijin Huang, John G. M. Adams and Yong Zhu *

Received 21st March 2017,
Accepted 8th April 2017

DOI: 10.1039/c7sm00568g

rsc.li/soft-matter-journal

Self-folding of a pre-strained shape memory polymer (SMP) sheet was demonstrated using local joule heating. Folding is caused by shrinkage variation across the thickness of the SMP sheet. The folding direction can be controlled by the interfacial interaction between the heater and the SMP sheet. When the heater is placed on the SMP sheet with no constraint (weak interface), the SMP sheet folds toward the heater. Temperature gradient across the SMP thickness gives rise to the shrinkage variation. By contrast, when the heater is fixed to the SMP sheet (strong interface), the SMP sheet can fold away from the heater. In this case shrinkage variation is dictated by the constraining effect of the heater. In either mode, 180 degrees folding can be achieved. The folding angle can be controlled by varying the heater width and folding time. This method is simple and can be used to fold structures with sharp angles in a sequential manner. A variety of structures were folded as demonstrations, including digital numbers 0–9, a cube, a boat, and a crane.

Introduction

The fabrication of three-dimensional (3D) structures and devices is of increasing interest. An attractive strategy is to transform two-dimensional (2D) sheets into 3D architectures.[1–6] One method is controlled compressive buckling of planar structures.[7–9] While ingenious, this method is challenging for fabricating structures with sharp angles and often requires sophisticated mechanics design. Another method is origami-inspired folding.[10,11] Various actuation mechanisms have been used to accomplish folding, including capillary force,[12] light-activated stress relaxation across the film thickness,[13] and a bimorph structure actuated by heat,[14] swelling,[15,16] or the electric field.[5]

Shape memory materials[11,17] especially shape memory polymers (SMPs)[18–20] have attracted much recent attention for origami folding. SMPs can respond to many types of stimuli, including light,[21] heat,[22–24] electricity,[25] moisture,[26] and pH change.[27] SMPs can be pre-strained with a uniform tensile strain across the thickness and the release of tensile strain above a threshold temperature gives rise to in-plane shrinkage. To convert the in-plane shrinkage of a SMP sheet to out-of-plane deformation, several methods have been developed. The first method used a bilayer structure,[28,29] *i.e.* bonding a SMP layer to an un-shrinkable layer. When heated, shrinkage of the SMP layer caused (continuous) bending of the bilayer toward the SMP side. In another method, a heater strip was sandwiched between a SMP layer and a structural layer.[1,30,31] Shrinkage of the SMP layer led to (localized) folding. In the third method, localized folding was achieved by generating a local gradient in shrinkage across the thickness of the SMP sheet.[32,33] As demonstrated by Liu *et al.*,[33] a temperature gradient across the thickness can be generated by local light absorption defined by a line pattern, leading to a gradient in shrinkage across the thickness. In the first two methods the heaters were fixed to the SMP sheets and the bending or folding was toward the SMP side, while in the third method there was no heater and the folding was toward the light (or away from the SMP side). In all three cases the folding angles were limited (*e.g.* <159 degrees for the second approach[30] and <110 degrees for the third approach[34]). It appears that the SMP-heater interface plays an important role in controlling the folding behavior. It is thus of relevance to understand such an interfacial interaction and explore whether the interaction can offer additional opportunities to control folding.

Here we report self-folding of a SMP sheet triggered by local joule heating using a flexible heater, focusing on the effect of the SMP-heater interface. We identified three modes of operation depending on the interfacial interaction (constraint) between the heater and the SMP sheet. In all modes, folding is caused by shrinkage variation across the thickness of the SMP sheet. When the heater is placed on the SMP sheet with no constraint (weak interface), the SMP sheet folds toward the heater. The shrinkage variation is caused by the temperature gradient across the

Department of Mechanical and Aerospace Engineering, North Carolina State University, Raleigh, North Carolina 27695-7910, USA. E-mail: yong_zhu@ncsu.edu

† Electronic supplementary information (ESI) available: Detailed experimental results and analysis (pdf), Video S1: folding process of number '6', Video S2: folding process of a crane. See DOI: 10.1039/c7sm00568g

thickness. By contrast, when the heater is fixed (glued) to the SMP sheet (total constraint or strong interface), the SMP sheet can fold away from the heater due to the constraining effect of the heater, *i.e.* the heater constrains the shrinkage of the SMP sheet on the interface side. In either mode, 180 degrees folding can be achieved. An intermediate mode with the heater delaminated from the SMP sheet along the interface but anchored at two edges (partial constraint) was also studied. As demonstrated, several structures including numbers from zero to nine, a cube, a boat and a crane were fabricated by folding.

Results and discussion

Three folding modes

Fig. 1a shows the experimental setup and Fig. 1b shows the schematic of a heater on the SMP sheet. The heater was fabricated by coating AgNWs on a polyimide (PI) sheet. The SMP sheet used was pre-strained polystyrene (PS). It is important to isolate the AgNW film from the PS by another layer (*e.g.* PI used here), which can keep the AgNW film mechanically stable during folding. If the AgNWs were directly coated on top of the PS sheet, large deformation of the PS sheet during folding would severely deform the AgNWs, leading to a significant resistance increase or even failure of the heater (Fig. S1, ESI†). The reason to choose PI as the heater substrate was its high thermal stability. The glass transition temperature of PI is 410 °C, much higher than the temperature required to fold PS (~140 °C). PI is a widely used substrate material for flexible heaters.[35] The AgNW/PI heater can reliably provide high temperature up to 160 °C (Fig. S2, ESI†). The power generated using the flexible heater is much more intense than that from the light absorption approach. For example, an infrared lamp typically provided 1 W cm^{-2} power[34] while Joule heating can provide up to 5 W cm^{-2} (*e.g.* in Fig. 5b).

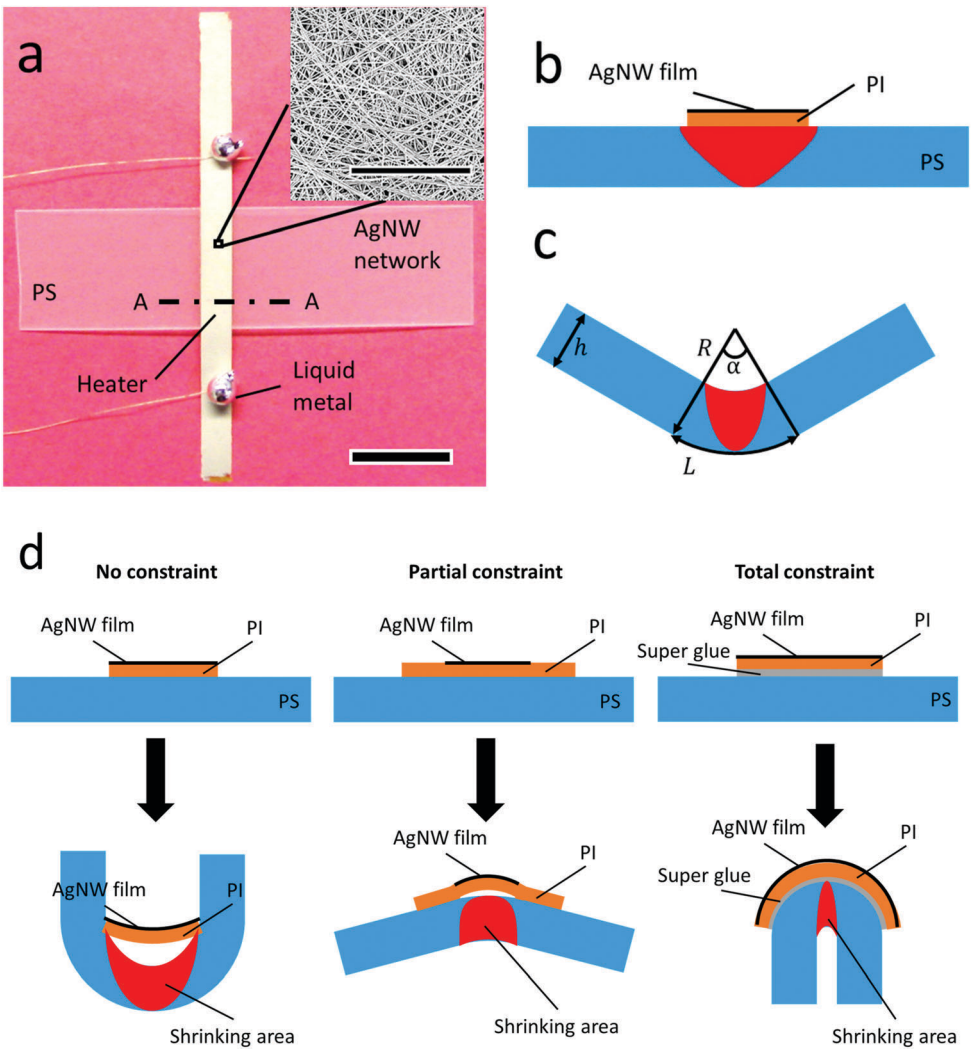

Fig. 1 (a) Experimental setup showing the pre-strained PS sheet and the flexible AgNW/PI heater on top. Scale bar: 10 mm. The inset shows the AgNW network (scale bar: 10 μm); (b) schematic of the cross section A–A in panel (a) and the temperature distribution in PS (according to FEA simulation). In the red area the temperature is above the threshold temperature for the shrinkage of PS; (c) schematic showing the folding geometry and related parameters; (d) schematics showing the three modes of operation for folding a PS sheet: no constraint, partial constraint and total constraint.

Thus folding can be realized without the need for a hot plate as in the light absorption approach.

Fig. 1b shows the steady-state temperature distribution in the PS sheet calculated using finite element analysis (FEA), assuming a constant temperature in the heater as the boundary condition (the constraining effect of the heater was neglected here). In the red area the temperature is above the threshold temperature (T_c) for the shrinkage of PS, which is taken as 140 °C here. It is known that the glass transition temperature (T_g) of PS is ~100 °C, but to achieve considerable shrinkage, the temperature needs to be higher.[28,34] When the temperature reaches above T_c, the PS sheet shrinks (releasing its pre-strain of 50%). Since the top side heats more, a temperature gradient across the thickness of the PS sheet develops, as shown in Fig. 1b. As a result, the top side shrinks more than the bottom side and hence the PS sheet tends to fold upward (assuming that the mechanical constraint of the heater is not significant). The folding angle is determined by the difference in the shrinkage of the two sides. The heated region bends to an arc, as shown in Fig. 1c. In an ideal case (best scenario), only the top surface shrinks by 50% while the bottom surface does not shrink. The folding angle (α) can be estimated by a simple geometric relationship,

$$\alpha = \frac{L}{R} = \frac{L/2}{R-h} \quad (1)$$

where L is the length of the heated area on the top surface before folding (*i.e.* approximately the heater width), R is the radius of curvature, and h is the thickness of the PS sheet (0.25 mm used in this study). According to eqn (1), $R = 2h$ and 180 degrees folding can be obtained when the heater width reaches 1.57 mm.

When the mechanical constraint is considerable, upward folding will be intervened due to resistance from the heater. The mechanical interaction between the heater and the PS substrate can be considered in three cases – no constraint, partial constraint and total constraint. A schematic showing the three corresponding modes of operation is shown in Fig. 1d. When the heater sits on top of the substrate with only weak adhesion like van der Waals interaction between them (*i.e.* no constraint), folding of the PS substrate can continue with sliding and delamination of the heater. When the adhesion is weak but both edges of the heater are anchored onto the substrate (*i.e.* partial constraint), shrinkage of the top surface of the substrate can cause buckle delamination of the heater. Without sliding of the heater, the resistance to folding becomes stronger, leading to the reduced folding angle and even folding away from the heater. When the heater is fixed to the substrate (*i.e.* total constraint), both sliding and buckle delamination are prevented and so is the shrinkage of the top surface of the substrate. Shrinkage of the bottom surface can cause folding away from the heater. Here we define folding toward the heater as inward folding, while folding away from the heater as outward folding. Note that the PI sheet used here is relatively stiff compared to the PS substrate. Otherwise the heater could wrinkle under compression and the AgNWs on top of the PI sheet might not survive such wrinkling.

Folding without constraint

In the case of no constraint (*e.g.* van der Waals interaction), the AgNW/PI heater was placed on top of the PS substrate. The heater can be peeled off after folding, leaving a clean folded structure. Fig. 2 shows the folding results. PS folded toward the heater (inward folding). The folding angle as a function of heater width is plotted in Fig. 2a. When the heater width was less than 1 mm, the maximum folding angle was less than 180 degrees and varied from sample to sample. Fig. S4 (ESI†) shows the inward folding for the heater width of 0.5 mm where the maximum folding angle was 140 degrees. Increasing heater

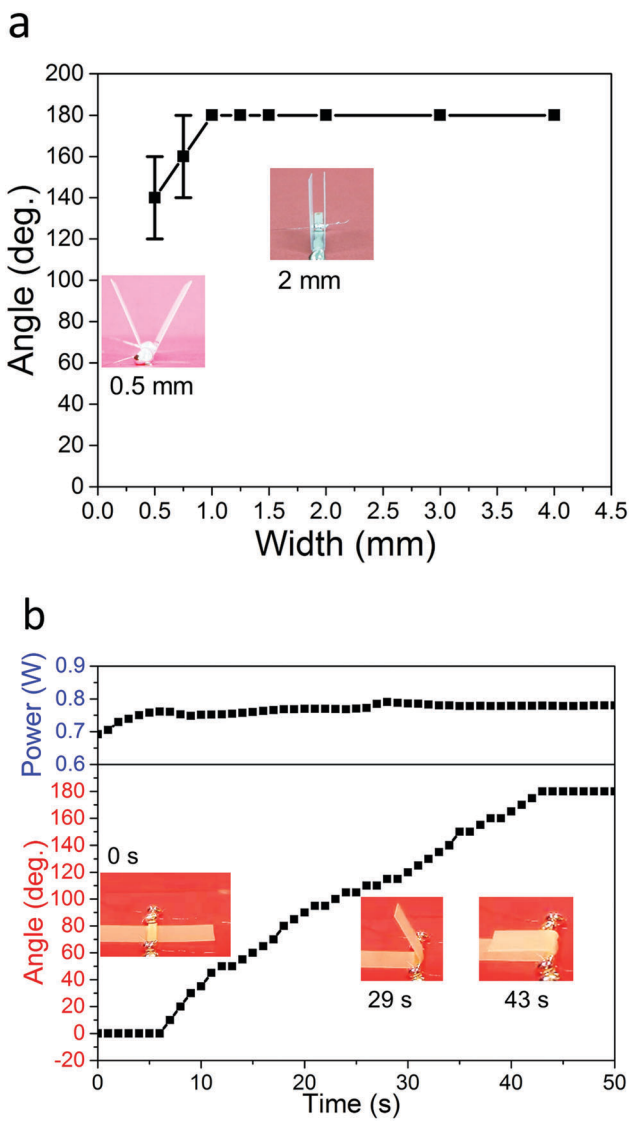

Fig. 2 Folding results in the case of no constraint. (a) Relationship between the inward folding angle and heater width. Insets are side views of the folded structures with 0.5 mm and 2 mm wide heaters; (b) time response and power input during inward folding with a 2 mm wide heater. Insets show several snapshots during folding.

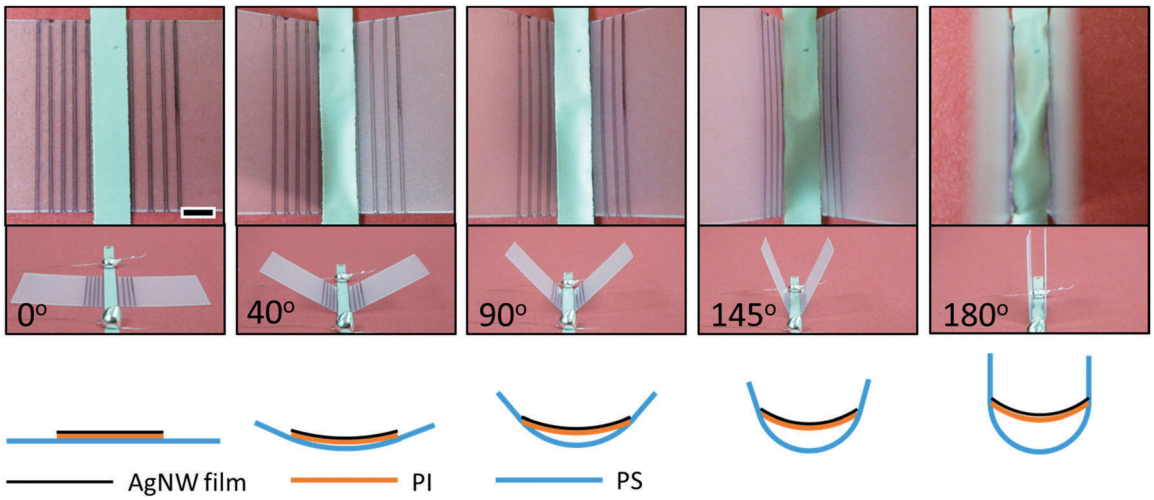

Fig. 3 Deformation of heater in the case of no constraint. Top: Top view; middle: side view; bottom: schematic of the cross section from side view. Scale bar: 2 mm. Folding was stopped by turning off the power supply. After taking images, folding was resumed by turning on the power supply.

width to 1 mm or wider led to complete folding, *i.e.* two ends of the PS sheet touched each other, which was denoted as 180 degrees in Fig. 2a. Fig. 3 shows the deformation of the heater during inward folding. Folding can be stopped by turning off the power supply and resumed by turning it back on. Black parallel lines were drawn on the PS sheet in order to show the relative position between the heater and the substrate. As shrinkage of the substrate began, edges of the heater slid on the substrate in order to accommodate the shrinkage, which can be seen by comparing the images at different folding angles in Fig. 3. For example, there were initially five black lines to the left of the heater. They became four when the substrate folded to 90 degrees, which indicated that the heater slid over one black line. As the substrate started to fold, the center of the heater started to delaminate from the substrate. This is shown schematically at the bottom of Fig. 3. During folding, the heater initially bent with the substrate, and then transited to sliding and delamination ("climbing" up along the folded substrate) to reduce the bending energy. Bending of the heater decreased its chord length, which can be measured from the top view of the heater. From the chord length and the folding angle (measured from the side view), the shape and position of the heater can be determined (Fig. S5–S7, ESI†).

As the heater climbed up and formed a gap between the heater and the substrate in the folded region, one question would be how did the folding process continue? Note that the two edges of the heater remained in contact with the substrate. With the heater sliding, more areas were heated (by edges of heater) and shrank, leading to progression of folding. As a result of sliding, a narrower heater width (*e.g.* 1 mm instead of 1.57 mm according to eqn (1)) was able to give 180 degrees folding, as shown in Fig. 2a. Moreover, the gap between the heater and the substrate can offer one additional advantage. Overheating of the folded region can cause unfolding as the bottom surface was also heated and shrank – see the case of the total constraint to be discussed later. Forming such a gap can prevent the overheating and unfolding of the folded region.

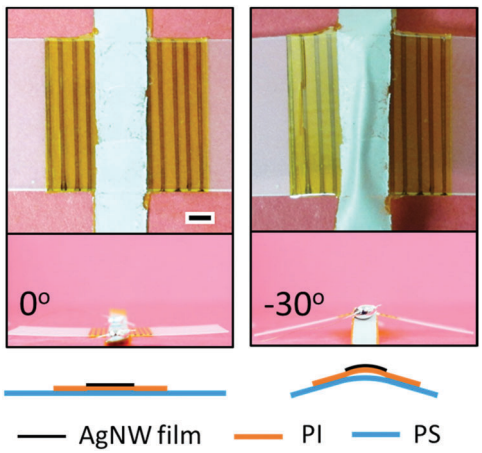

Fig. 4 Deformation of heater in the case of partial constraint. Top: Top view; middle: side view; bottom: schematic of the cross section from the side view. Scale bar: 2 mm.

Folding with partial constraint

In the case of partial constraint (*i.e.* no sliding), inward folding was resisted by the heater. Fig. 4 shows folding with a bare tape on each edge of the heater to prevent sliding of the heater. Shrinkage of the top side of the PS compressed the heater and caused buckle delamination. The resistance force from the heater opposed the shrinkage of the top side of the PS. Only two anchored edges of the heater can heat up the PS sheet, which however cannot slide as in the case of no constraint. As a result shrinkage of the top side of the PS was limited. When the PS sheet was heated through, heating of the backside of the PS sheet can cause shrinkage of the backside, which soon surpassed that of the top side, leading to outward folding. The outward folding angle was quite small in this case, as shown in Fig. 4 and Fig. S8 (ESI†). Note that if only one edge of the heater is constrained, the heater can still slide but with reduced delamination (climb) compared to the case of no

constraint. As a result, 180 degrees folding was still achievable (Fig. S9, ESI†).

Folding with total constraint

The outward folding angle in the case of partial constraint was limited because the shrinkage of the top surface was not completely prevented. It is thus of interest to explore the folding behavior in the case of total constraint, that is, delamination is also prevented in addition to sliding (*e.g.* by gluing the heater to the substrate). The folding angle was found to depend on the heater width (Fig. 5a). Note that the positive angle corresponds to inward folding, while the negative angle corresponds to outward folding. With a narrow heater, inward folding still occurred but the folding angle was smaller than that in the first case (no constraint). The inward folding angle decreased with increasing heater width. At the heater width of ~0.75 mm, outward folding took over and the outward folding angle increased upon increasing the heater width up to ~1.5 mm where 180 degree outward folding was obtained.

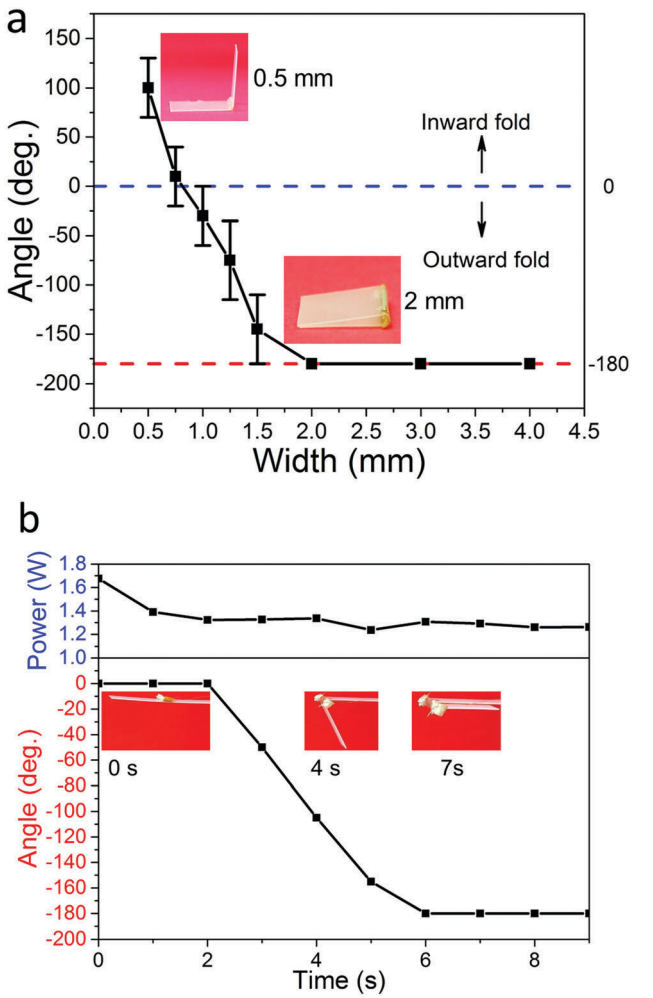

Fig. 5 Folding results in the case of total constraint. (a) Relationship between the folding angle and heater width. Insets are side views of the folded structures with 0.5 mm and 2 mm wide heaters; (b) time response and power input during outward folding with a 2 mm wide heater. Insets show several snapshots during folding.

The folding behavior in this case was dictated by the temperature distribution in the PS sheet. FEA shows that the heated area above T_c on the top surface was slightly wider than the heater width (the extra heated area was nearly constant, regardless of the heater width) (Fig. S10 and S11, ESI†). The heater was assumed to be stiff compared to the PS and not deformed under compression during folding. For a narrow heater, the extra heated area on the top surface was larger than the heated area on the bottom surface, leading to inward folding. For a wide heater, the extra heated area on the top surface was smaller than the heated area on the bottom surface, leading to outward folding. Fig. S12a (ESI†) shows inward folding for a heater width of 0.5 mm. The inset shows mass accumulation adjacent to the heater, which indicates shrinkage of the extra heated area mentioned above. Fig. S12b (ESI†) shows the outward folding for a heater width of 2 mm. The inset shows that the heater was in close contact with the PS. No wrinkles or buckle delamination can be observed, confirming that the heater was not deformed. This scenario can be viewed as the opposite of that described by eqn (1) – the bottom surface shrank by 50% (under the heater) while the top surface did not shrink. As predicted by eqn (1), 180 degrees outward folding can be achieved with a heater width ~1.57 mm, in good agreement with the experimental results (Fig. 5a). Also the bending of this bilayer structure (PS substrate and AgNW/PI heater) can be analyzed using a bimorph model (see details in the Bimorph model analysis section in the ESI†), which calculates a heater width of ~1.58 mm to achieve 180 degrees outward folding.

Time response of folding

Fig. 2b and 5b show the time responses of two representative samples corresponding to the first and third cases discussed above – no constraint and total constraint, respectively. A heater width of 2 mm was used in both cases. A constant current was applied to the heater while the voltage was monitored during the folding process. In the case of no constraint (Fig. 2b), inward folding occurred. The folding started at 7 s after turning on the heater and stopped at 43 s with the folding angle of 180 degrees. The input power increased from 0.75 W to 0.8 W. The heating area was ~0.25 cm^2 and the power density was about 3 W cm^{-2}. In the case of total constraint (Fig. 5b), outward folding occurred. The folding started at ~2 s after turning on the heater and stopped at ~6 s with the folding angle of 180 degrees, much faster than the previous case. The input power decreased from 1.6 W to 1.3 W. The heating area was ~0.25 cm^2 and the power density was close to 5 W cm^{-2}. Fig. S14 (ESI†) shows the time responses of two additional samples to demonstrate the reproducibility of folding. In both cases, resistances of the AgNW films slightly changed before folding started and remained nearly constant during folding. The resistance change occurred as the temperature ramped up until reaching T_c for folding to start, which can be attributed to several factors. For inward folding, the increase of resistance

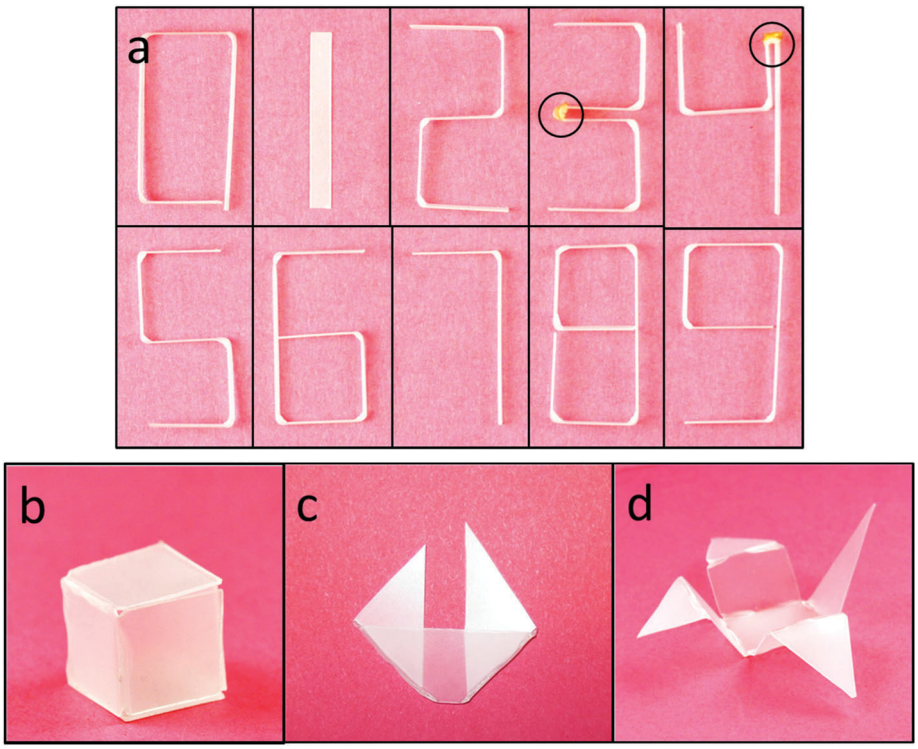

Fig. 6 Structures folded with the AgNW/PI heaters. (a) Digital numbers (black circles indicate complete outward folding); (b) a cube folded by inward folding (the heater was peeled off); (c) a simple sailing boat folded by 180 degrees inward folding (heater was peeled off); (d) a crane folded by inward folding (the heater was peeled off).

might be due to thermal expansion of the PI sheet,[36] and/or reduced conductivity of Ag at elevated temperatures. In the case of outward folding where higher input power was used, the decrease of resistance might be caused by the annealing effect, which become dominant at high temperature.[37] In the case of total constraint, the PS sheet was heated thoroughly before folding started to occur. That is why a higher input power was needed. The nearly constant resistances during folding indicated reliable heater performances in both cases.

Comparison with other folding methods for SMP

Now we can compare our method with the three methods for folding SMPs as mentioned in the Introduction. Wang *et al.* combined a SMP sheet with a rigid heater to make a bimorph structure.[28] However, they covered the whole area of the SMP with another layer, thus the bimorph structure tended to wrap together instead of forming a sharp angle. In our case, sharp folding can be achieved due to the triggering of a local heater that serves as a hinge for folding. Wood and co-workers folded various structures using a local heater.[1,30,31] Their method is similar to our total-constraint case but with several differences: (1) they used three layers (SMP, a heater and an additional rigid layer), while we used only a SMP and heater layers; (2) their heater (Cu trace) was fabricated by lithography involving printing a mask and etching, while our AgNW heater was drop casted using a stencil; (3) their maximum folding angle reported was 159 degrees while we could routinely achieve 180 degrees. On the other hand, the light-triggered local folding of a SMP by Liu *et al.* is similar to our no-constraint case. Their method is simple, but the delivered power was relatively low (*e.g.* the SMP sheet has to be placed on a hot plate to facilitate folding[33,34]). Also it is quite challenging to achieve sequential folding using their method.[38,39]

Folded structures

To demonstrate the application of joule heating induced folding of SMPs, several structures were obtained by folding different hinges sequentially. Folding can be stopped at the desired angle by turning off the current. Fig. 6 shows several structures folded by inward and/or outward folding. Fig. 6a shows digital numbers. 90 degrees folding was achieved by inward folding (heaters was peeled off). 180 degrees folding (highlighted by black circles) was achieved by outward folding. Fig. 6b shows a cube by inward folding (tiny notches are cut at the corner to make room for the heater). Fig. 6c shows a simple sailing boat by 180 degrees inward folding (the heater was peeled off). Fig. 6d shows a crane folded by inward folding (the heater was peeled off). Video S1 (ESI†) shows the folding process of number '6', while Video S2 (ESI†) shows folding of a crane.

Conclusion

In summary, we reported self-folding of pre-strained PS sheets triggered by local joule heating using flexible AgNW/PI heaters (with AgNW networks on top of PI sheets). Folding was caused

by the temperature gradient across the thickness of a PS sheet. The folding behavior was found to depend on the mechanical interaction between the heater and the PS sheet. In the case of no constraint (weak interface between the heater and the PS sheet), the PS sheet folded toward the heater with the heater sliding and climbing up along the PS sheet. 180 degrees inward folding was achieved with the heater width of over 1 mm. In the case of partial constraint (*i.e.* the heater delaminated from the PS sheet along the interface but fixed at two edges), inward folding was resisted and outward folding became possible. In the case of total constraint (*i.e.* the heater fixed to the PS), inward folding transited to outward folding with increasing heater width. 180 degrees outward folding was achieved with the heater width of over 1.5 mm. Several structures including numbers from zero to nine, a cube, a boat and a crane were folded using inward and/or outward folding. The method is simple and can be used to fold structures with sharp angles in a sequential manner. The effect of interfacial interaction studied in this work can be extended to other folding mechanisms triggered by stimuli that are in contact with the structures to be folded.

Materials and methods

Materials

A commercially available SMP with the brand name of Shrinky Dinks was used in this study, which is made of pre-strained PS. The PS sheet was cut into 12 mm stripes. The thickness was 10 mil (0.25 mm). Biaxial tensile strain is incorporated into the SMP sheet, which is uniform across the thickness. The PS sheet shrinks in plane by 50% in both directions upon relaxation above T_c (140 °C). The PI sheet was purchased from CAPLINQ with a thickness of 1 mil (0.025 mm). The PI sheet can be cut into stripes with desired widths. Super glue was purchased from amazon under the name of Loctite Liquid Professional Super Glue 20-Gram Bottle.

Sample preparation

The heater was fabricated by coating silver nanowires (AgNWs) onto the PI sheet. AgNWs were synthesized following a standard approach.[40] The PI sheet was taped onto a clean glass slide, while AgNWs dispersed in ethanol were dropped casted on top of PI. A Mayer Rod was used to make a uniform coating. Thermal treatment at 50 °C was conducted to evaporate the ethanol. Then the AgNW/PI heater was peeled off from the glass slide and put onto PS stripes. For the case of partial constraint, a wide PI sheet was taped on the PS stripe (in perpendicular direction). The heater was fabricated by coating AgNWs in the central region (two edges were masked), leaving bare tape along each edge. For the case of total constraint, super glue was used to glue the heater onto the PS sheet.

Folding experiments

Agilent 6613C power supply was used to apply the current. Voltage was monitored using an Agilent 34401A digital multimeter. Thin copper wires were used to connect the heater to the power supply. Liquid metal or silver paste was used for the reliable contact between the copper wire and the heater. Two cameras were used to take images during the folding processes, one for top view, and the other for side view. For the top view, the distance between the camera and the sample was kept constant.

Acknowledgements

The authors acknowledge financial support from the National Science Foundation (NSF) through Award No. EFRI-1240438. The authors would like to thank Professors J. Genzer and M. D. Dickey for discussions.

References

1 S. Felton, M. Tolley, E. Demaine, D. Rus and R. Wood, *Science*, 2014, **345**, 644–646.
2 R. Fernandes and D. H. Gracias, *Adv. Drug Delivery Rev.*, 2012, **64**, 1579–1589.
3 X. Guo, H. Li, B. Y. Ahn, E. B. Duoss, K. J. Hsia, J. A. Lewis and R. G. Nuzzo, *Proc. Natl. Acad. Sci. U. S. A.*, 2009, **106**, 20149–20154.
4 T. G. Leong, B. R. Benson, E. K. Call and D. H. Gracias, *Small*, 2008, **4**, 1605–1609.
5 J. Shintake, S. Rosset, B. Schubert, D. Floreano and H. Shea, *Adv. Mater.*, 2016, **28**, 231–238.
6 Z. M. Song, T. Ma, R. Tang, Q. Cheng, X. Wang, D. Krishnaraju, R. Panat, C. K. Chan, H. Y. Yu and H. Q. Jiang, *Nat. Commun.*, 2014, **5**, 3140.
7 S. Xu, Z. Yan, K. I. Jang, W. Huang, H. R. Fu, J. Kim, Z. Wei, M. Flavin, J. McCracken, R. Wang, A. Badea, Y. Liu, D. Q. Xiao, G. Y. Zhou, J. Lee, H. U. Chung, H. Y. Cheng, W. Ren, A. Banks, X. L. Li, U. Paik, R. G. Nuzzo, Y. G. Huang, Y. H. Zhang and J. A. Rogers, *Science*, 2015, **347**, 154–159.
8 Y. H. Zhang, Z. Yan, K. W. Nan, D. Q. Xiao, Y. H. Liu, H. W. Luan, H. R. Fu, X. Z. Wang, Q. L. Yang, J. C. Wang, W. Ren, H. Z. Si, F. Liu, L. H. Yang, H. J. Li, J. T. Wang, X. L. Guo, H. Y. Luo, L. Wang, Y. G. Huang and J. A. Rogers, *Proc. Natl. Acad. Sci. U. S. A.*, 2015, **112**, 11757–11764.
9 Z. Yan, F. Zhang, J. C. Wang, F. Liu, X. L. Guo, K. W. Nan, Q. Lin, M. Y. Gao, D. Q. Xiao, Y. Shi, Y. T. Qiu, H. W. Luan, J. H. Kim, Y. Q. Wang, H. Y. Luo, M. D. Han, Y. G. Huang, Y. H. Zhang and J. A. Rogers, *Adv. Funct. Mater.*, 2016, **26**, 2629–2639.
10 P. Wang-Iverson, R. J. Lang and M. Yim, *Origami 5 Fifth International Meeting of Origami Science, Mathematics, and Education*, CRC Press, Boca Raton, 2011.
11 E. Hawkes, B. An, N. Benbernou, H. Tanaka, S. Kim, E. Demaine, D. Rus and R. Wood, *Proc. Natl. Acad. Sci. U. S. A.*, 2010, **107**, 12441–12445.
12 C. Py, P. Reverdy, L. Doppler, J. Bico, B. Roman and C. N. Baroud, *Phys. Rev. Lett.*, 2007, **98**, 156103.

13 J. Ryu, M. D'Amato, X. Cui, K. N. Long, H. J. Qi and M. L. Dunn, *Appl. Phys. Lett.*, 2012, **100**, 161908.
14 E. Smela, O. Inganas and I. Lundstrom, *Science*, 1995, **268**, 1735.
15 J. H. Na, A. A. Evans, J. Bae, M. C. Chiappelli, C. D. Santangelo, R. J. Lang, T. C. Hull and R. C. Hayward, *Adv. Mater.*, 2015, **27**, 79–85.
16 G. Stoychev, S. Zakharchenko, S. B. Turcaud, J. W. Dunlop and L. Ionov, *ACS Nano*, 2012, **6**, 3925–3934.
17 K. Otsuka and C. M. Wayman, *Shape memory materials*, Cambridge University Press, New York, 1998.
18 Q. Zhao, W. Zou, Y. Luo and T. Xie, *Sci. Adv.*, 2016, **2**, e1501297.
19 Y. Liu, J. Genzer and M. D. Dickey, *Prog. Polym. Sci.*, 2016, **52**, 79–106.
20 Q. Zhao, H. J. Qi and T. Xie, *Prog. Polym. Sci.*, 2015, **49**, 79–120.
21 A. Lendlein, H. Y. Jiang, O. Junger and R. Langer, *Nature*, 2005, **434**, 879–882.
22 A. Lendlein and S. Kelch, *Angew. Chem., Int. Ed.*, 2002, **41**, 2035–2057.
23 Y. Liu, K. Gall, M. L. Dunn and P. McCluskey, *Mech. Mater.*, 2004, **36**, 929–940.
24 Q. Zhang, J. Wommer, C. O'Rourke, J. Teitelman, Y. Tang, J. Robison, G. Lin and J. Yin, *Extreme Mech. Lett.*, 2016, **11**, 111–120.
25 J. W. Cho, J. W. Kim, Y. C. Jung and N. S. Goo, *Macromol. Rapid Commun.*, 2005, **26**, 412–416.
26 W. Huang, B. Yang, L. An, C. Li and Y. Chan, *Appl. Phys. Lett.*, 2005, **86**, 114105.
27 X. J. Han, Z. Q. Dong, M. M. Fan, Y. Liu, Y. F. Wang, Q. J. Yuan, B. J. Li and S. Zhang, *Macromol. Rapid Commun.*, 2012, **33**, 1055–1060.
28 H. Wang, Y. Wang, B. C. K. Tee, K. Kim, J. Lopez, W. Cai and Z. Bao, *Adv. Sci.*, 2015, **2**, 1500103.
29 M. T. Tolley, S. M. Felton, S. Miyashita, D. Aukes, D. Rus and R. J. Wood, *Smart Mater. Struct.*, 2014, **23**, 094006.
30 S. Felton, K. Becker, D. Aukes and R. Wood, *J. Micromech. Microeng.*, 2015, **25**, 085004.
31 S. M. Felton, M. T. Tolley, B. Shin, C. D. Onal, E. D. Demaine, D. Rus and R. J. Wood, *Soft Matter*, 2013, **9**, 7688–7694.
32 D. Davis, B. Chen, M. D. Dickey and J. Genzer, *J. Mech. Robot.*, 2016, **8**, 031014.
33 Y. Liu, J. K. Boyles, J. Genzer and M. D. Dickey, *Soft Matter*, 2012, **8**, 1764–1769.
34 Y. Liu, R. Mailen, Y. Zhu, M. D. Dickey and J. Genzer, *Phys. Rev. E: Stat., Nonlinear, Soft Matter Phys.*, 2014, **89**, 042601.
35 Q. Huang, W. Shen, X. Fang, G. Chen, J. Guo, W. Xu, R. Tan and W. Song, *RSC Adv.*, 2015, **5**, 45836–45842.
36 X. Y. Zeng, Q. K. Zhang, R. M. Yu and C. Z. Lu, *Adv. Mater.*, 2010, **22**, 4484–4488.
37 T.-B. Song, Y. Chen, C.-H. Chung, Y. Yang, B. Bob, H.-S. Duan, G. Li, K.-N. Tu, Y. Huang and Y. Yang, *ACS Nano*, 2014, **8**, 2804–2811.
38 Y. Lee, H. Lee, T. Hwang, J.-G. Lee and M. Cho, *Sci. Rep.*, 2015, **5**, 16544.
39 Y. Mao, K. Yu, M. S. Isakov, J. Wu, M. L. Dunn and H. J. Qi, *Sci. Rep.*, 2015, **5**, 13616.
40 Y. Sun, Y. Yin, B. T. Mayers, T. Herricks and Y. Xia, *Chem. Mater.*, 2002, **14**, 4736–4745.

